Does the correlation between Schmorl's nodes and vertebral morphology extend into the lumbar spine?

Journal:	*American Journal of Physical Anthropology*
Manuscript ID:	AJPA-2014-00328.R2
Wiley - Manuscript type:	Technical Note
Date Submitted by the Author:	n/a
Complete List of Authors:	Plomp, Kimberly; Simon Fraser University, Archaeology Roberts, Charlotte; Durham University, Archaeology Strand Vidarsdottir, Una; University of Iceland, Biomedical Center
Key Words:	Disc herniation, geometric morphometrics, shape analysis, palaeopathology
Subfield: Please select your first choice in the first field.:	Human biology [living humans; behavior, ecology, physiology, anatomy], Bioarchaeology [including forensics]

Technical Note: Does the correlation between Schmorl's nodes and vertebral morphology extend into the lumbar spine?

Abstract:

Schmorl's nodes are depressions on vertebrae due to herniation of the nucleus pulposus of the intervertebral disc into the vertebral body. This study provides an extension of our previous study which analyzed the shape of the lower thoracic spine and found that vertebral morphology was associated with the presence of Schmorl's nodes. Ninety adult individuals from the late Medieval site of Fishergate House, York, and the Post-Medieval site of Coach Lane, North Shields, Tyne and Wear, England, were analysed using 2D geometric morphometrics to identify possible relationships between vertebral morphology and Schmorl's nodes at the thoraco-lumbar junction and in the lumbar spine. A significant correlation was found between vertebral shape and the presence of Schmorl's nodes in twelfth thoracic vertebrae and lumbar vertebrae 1-3. The findings corroborate previous findings and suggest that vertebral shape may be an important factor in spinal health and it is hypothesized that the pedicle shape of affected vertebrae may not provide adequate structural support for the vertebral bodies, resulting in vertical disc herniation.

Keywords Disc herniation; geometric morphometrics; shape analysis; palaeopathology

Introduction

Schmorl's nodes are lesions that result from vertical herniation of the nucleus pulposus of the intervertebral disc. They can be recognized by the presence of a depression on the surface of the vertebral body (Schmorl and Junghans, 1971; Pfirrmann and Resnick, 2001). They most frequently affect the lower thoracic and lumbar spine and are common in both living and past populations, with prevalence rates ranging from 5-77% depending on the sample studied and recording protocol used (Pfirrmann & Resnick 2001; Dar et al. 2009; Mok et al. 2010; Novak & Šlaus 2011; Robb et al. 2001; Üstündağ 2009). The exact aetiology of intervertebral disc herniation, including those that result in Schmorl's nodes, continues to elude researchers. However, the general consensus is that their cause is multi-factorial, with genetic predisposition, developmental problems, a specific disc composition, and physical strain or trauma to the spine identified as the main contributory factors influencing their development (Adams and Dolan, 2012; Burke, 2012; Dar et al., 2010; Mok et al., 2010; Williams et al., 2007; Von Forell et al., 2014).

Previous research has indicated that the morphology of vertebrae may be associated with the occurrence of intervertebral disc herniation. For example, Harrington et al.'s (2001) study on the size and form of the vertebrae of the lower lumbar spine found that larger vertebral bodies in males, and circular vertebral bodies in both males and females, were more prone to experiencing disc herniation. More recently, Plomp et al. (2012) found a significant correlation between the morphology of the vertebral body, neural canal, and pedicles and the presence of Schmorl's nodes in the lower thoracic spine (T10-T12). The present paper aims to expand upon our previous study of thoracic vertebrae. To achieve this aim, we analyzed the thoraco-lumbar junction and lumbar spine to investigate if the morphological association found in the lower

thoracic spine also exists lower down the spine (Plomp et al., 2012). If a relationship is found, it would provide further support for the hypothesis that vertebral morphology is correlated with the development of Schmorl's nodes.

Materials and Methods

The study sample was composed of a total of 369 vertebrae, including the twelfth thoracic and the first to fourth lumbar vertebrae. These vertebrae represent the lower spines of 90 adult individuals from the cemetery sites of Fishergate House, York, dated to the 12^{th}-16^{th} centuries AD, and Coach Lane, North Shields, Tyne and Wear, dated to 1711-1857 AD (49 males, 35 females, 6 undetermined sex) (Table 1) (Holst, 2005; Langthorne, 2012). Analyses included vertebrae without Schmorl's nodes, termed 'healthy', as well as those exhibiting Schmorl's nodes, termed 'affected'. The inclusion of the twelfth thoracic vertebra in this study allowed for direct comparison of vertebral shapes previously identified in the lower thoracic spine (Plomp et al., 2012). The number of vertebrae in each dataset varied depending on bone preservation and consequently which landmarks were available for analysis (Table 2). Standard osteological analyses had previously been performed to determine sex and age at death (Brooks and Suchey, 1990; Bass, 1987; p12-25; Işcan et al., 1984, 1985; Lovejoy et al., 1985; Ascádi and Nemeskéri, 1970: p73-134; Phenice, 1969; Brothwell, 1981: p59-70) and this information was extracted from the archaeological site reports (Holst 2005; Langthorne 2012). Stature was estimated based on long bone lengths using the method of Trotter and Gleser (1958) in order to investigate the relationship between the presence of Schmorl's nodes and the size of the individual.

Schmorl's nodes were recorded on both superior and inferior vertebral body surfaces, all being healed remodelled lesions (Figure 2). Using the methodology of our first paper, Plomp et al. (2012), Schmorl's nodes were categorized as either a stage 1 or stage 2 lesion, based on the size of the lesion (Knüsel et al. 1997). Geometric morphometric techniques were used to quantify and compare vertebral shape (O'Higgins and Jones, 1998). Eight two-dimensional homologous landmarks and nine semi-landmarks, capturing the superior margins of the vertebrae, were digitized from standardised photographic images using TPSdig© software (Rohlf, 2004) (Figure 3). Semi-landmarks lack homology and were placed evenly along the external curve of the vertebral body (Bookstein, 1997). In order to minimize the shape differences related to spacing of the semi-landmarks, they were slid along the tangent plane to minimize bending energy of deformation (for full explanation, see Bookstein, 1997).

Once the data were acquired, they were tested for outliers using a Mahalanobis Distances in MorphoJ (Klingenberg 2011). No outliers were identified in the data. The data were then superimposed using generalized Procrustes analysis (GPA), which removed rotational and translational variation, as well as scaled the landmark configurations to centroid size (Bookstein, 1997; Goodall, 1991; Rohlf, 2003; Rohlf and Slice, 1990; Slice, 2007). Centroid size, the square root of the sum of the squared distances of each landmark from the centroid of the landmark configuration, was used as the measure of size and retained as an independent variable (O'Higgins and Jones, 1998; Zelditch et al. 2004).

The superimposed data were then subjected to principal components analyses (PCA), which illustrate patterns of shape variability within the sample. Principal component (PC) scores were assessed using the Shapiro-Wilks test for normality and Levene's test for equality of variance; the data were found to be normally distributed with equal variance between groups.

Outliers were tested for using the Shapiro-Wilks test in SPSS© and were not found to influence the data and therefore outliers were not removed. After PCA, discriminant function analysis (DFA) with leave-one-out cross-validation was used to establish the power of discrimination between groups within the sample (Cardini et al., 2009; Kimmerle et al., 2008; White and Ruttenberg, 2007). To minimize noise from higher components, the number of PCs included in the cross-validated DFA was reduced using the method proposed by Baylac and Frieβ (2005), and cross-validated DFA scores were tested against over-fitting by randomization, as described by Kovarovic et al. (2011), with only scores above chance reported.

Finally, MANOVA tests were used to determine the statistical significance of differences in PC scores between the sexes, populations, and healthy and affected vertebrae. Hotelling t-tests were used to determine the difference in centroid size and stature between groups (i.e. sex, vertebral status). Chi-squared (χ^2) tests were used to determine statistical significance of the frequency of Schmorl's nodes. Unlike the previous study, there was no statistical difference ($p>0.529$) in shape between vertebrae with different stages of lesions, and therefore all affected vertebrae were analysed as a single group.

Intra-observer error was performed by comparing the greatest Procrustes distance between repeated observations with the smallest distance between other vertebrae. The greatest distance between the repeated observations was half the smallest distance between different vertebrae, which indicates that intra-observer error is unlikely to affect the classification of groups within the data (Bienvenu et al., 2011; Lieberman et al., 2007; Neubauer et al., 2009, 2010). Statistical analyses were performed in Morphologika© (O'Higgins and Jones, 2006), R (R Development Core Team), and SPSS® 16.0 (Inc., Chicago, IL).

Results

The number of affected L5 (n=2) vertebrae was too small to be considered for statistical analyses and only L1-4 vertebrae could be analysed. MANOVAs performed on PC scores found that there was no statistical difference between the two populations, Fishergate House and Coach Lane ($p>0.108$), and therefore the populations were treated as a homogenous group. There was no difference in stature between individuals with and without Schmorl's nodes ($p<0.504$). Affected vertebral bodies were significantly larger than their healthy counterparts ($p<0.05$) in all vertebrae analysed, except for the L4. Neural canal size was not significantly different between healthy and affected vertebrae ($p>0.555$), or between males and females ($p>0.202$). Males had on average larger vertebral bodies than females, although this was only statistically significant for T12 and L4 ($p<0.005$). Males were affected more often than females, with 55.1% of males and 40.0% of females having a node on at least one vertebra, although this difference was not significant (χ^2 $p=0.092$). Sexual dimorphism did not have a statistically significant effect on shape ($p>0.067$), and as centroid size is an independent variable that was excluded from further analyses, all subsequent shape analyses were based on pooled sex datasets. There was no significant difference in the occurrence of Schmorl's nodes with age (χ^2 $p=0.523$).

Figure 4 illustrates the differences between the mean shapes of healthy and affected vertebrae. Figure 5 illustrates the PCA plot showing the shape variance of healthy and affected T12-L4 vertebrae, with the mean of each group superimposed to simplify the plot for ease of interpretation. PC2 represents the shape difference of individual vertebrae and there is a clear separation of affected and healthy vertebrae means on PC3 (7.2% total variance). The wireframe images illustrate the shape differences occurring along PC3, with the reference shape representing the shape at the negative end of PC3 and the target shape representing the shape at the positive end. The main shape differences that occur, moving from the healthy vertebrae on

the negative end of PC3 to the affected vertebrae on the positive end, relate to a decrease in neural foramen size relative to the vertebral body, a posterior translation of the posterior margin of the vertebral body, and a widening and shortening of the pedicles. These changes result in affected vertebrae having relatively wider, shorter pedicles compared to healthy vertebrae, and the posterior margin of the vertebral body encroaching into the neural canal, resulting in a relatively more circular vertebral body in those affected when compared to a more heart-shaped body in healthy vertebrae.

After the PCA was performed on the landmark data, the PC scores were analysed with cross-validated DFA. Table 3 summarises the results of the cross-validated DFA on PC scores for each vertebra from T12 to L4 using 17 landmarks. The best discrimination between healthy and affected was found in T12, L1, and L2. Table 4 summarizes the results of MANOVAs performed on the PCs included in each DFA (reported in Table 3). Using 17 landmarks, statistical differences in shape between healthy and affected vertebrae could be identified in all vertebrae except L4 (Table 4).

To increase sample size, analyses were repeated using only the eight landmarks of the neural foramen and pedicles (Table 5), the anatomy of which had been shown to differ between healthy and affected vertebrae in the analyses of the full dataset. Figure 6 illustrates the shape variance of group means, with affected vertebrae residing on the negative end of PC3, and healthy vertebrae tending to reside on the positive end of PC3. The shape differences occurring from positive to negative PC3 were, again, a posterior translation of the posterior margin of the vertebral body and a shortening of the pedicles. Decreasing the number of landmarks generally decreased the power of the discriminant function, although T12 to L3 still display accuracies of over 70% for identifying healthy and affected vertebrae. With this landmark set, all vertebrae

showed a statistical difference in shape between vertebrae with Schmorl's nodes and those without (Table 4).

Discussion

The results indicate a relationship between the morphology and size of vertebrae and the presence of Schmorl's nodes in T12 and L1 to L3. The morphology of the lumbar spine, with the exception of L4, which only showed statistical significance in the eight landmarks set, is strongly correlated with the presence of Schmorl's nodes. The highest DFA scores were found in T12 and L1 (81.0% and 78.2%) for classifying affected and healthy vertebrae. These results support our previous findings and indicate that the shape characteristics identified in affected lumbar vertebrae are similar to those identified in affected T10 to T12 vertebrae (Plomp et al., 2012).

There was no difference found in vertebral shape of the lumbar spine relating to the extent of the lesions, as was identified in our previous work (Plomp et al. 2012). It may be possible that vertebral shape influences the severity of the lesions differently in the lumbar and thoracic regions of the spine. However, both the current and previous study included T12 vertebrae, but the resulting data were not consistent between the two studies. Plomp et al. (2012) found that vertebral shape differed between 12th thoracic vertebrae with stage 1 and stage 2 lesions, but the current study did not find this relationship. Therefore, it is likely that the relationship identified previously was a consequence of the populations, in terms of skeletal variation and gene pools, included in the analyses and that vertebral shape may not impact the size and depth of Schmorl's nodes. This area of inquiry would benefit from further research.

Figures 4 and 5 illustrate how affected and healthy group means separate based on shape variables illustrated on PC3, which represent 7.2% of the total shape variance for the 17

landmark set and 2.4% for the eight landmark set. This indicates that the shape differences associated with affected vertebrae are similar in T12 and L1-L3. The most apparent shape differences occurring along PC3 from healthy to affected vertebrae are a relative decrease in neural foramen size relative to the vertebral body, and a relative shortening of the pedicles. The group means represent a reduced variance that best discriminates between these groups, and the actual variance shows overlap between the groups. However, our results do suggest that the general morphological trends occurring in affected vertebrae are similar from T12 to L3 and are consistent throughout the lower spine, even between transitional and non-transitional vertebrae.

The morphology of affected vertebrae in the lumbar spine illustrated in Figure 3 is similar to that of affected vertebrae in the lower thoracic spine identified in T10 to T12 vertebrae (Plomp et al., 2012). These shape differences result in affected vertebrae having relatively rounder vertebral bodies, smaller neural foramina relative to the vertebral body, and shorter, wider pedicles. Additionally, the centroid size of the vertebral body was found to be larger in affected vertebrae, which would add to the relative size difference between the vertebral body and the posterior elements. Stature was not a significant determinant for the presence of Schmorl's nodes, indicating that it is the size of the vertebral body, and not the stature of the individual, that influences the development of the lesions.

Possible explanations for the correlation between vertebral size, this particular vertebral shape, and Schmorl's nodes have been discussed in our previous paper (Plomp et al. 2012), including the invocation of LaPlace's law on the larger, rounder vertebral bodies (Harrington et al., 2001; Letić 2012). LaPlace's law states that the ability for a fluid filled tube to resist tension is decreased with an increasing radius (Letić 2012). If the intervertebral disc is considered to be a fluid filled tube, the affected vertebrae would have larger, rounder discs and therefore a lower

resistance to tension (Harrington et al., 2001; Plomp et al. 2012). This hypothesis is also supported by the findings of Peloquin et al. (2014). The authors found that larger intervertebral discs are correlated with degeneration, although they conclude that this relationship could be a result of larger discs being more susceptible to degeneration or that degeneration increases the disc size (Peloquin et al. 2014). The pedicles transmit compressive loads from the vertebral body to the posterior elements and provide buttressing support for the vertebral body during spinal compression (Shapiro 1993a,b; Whyne et al. 1998; El-Khoury & Whitten 1993). Hongo et al. (1999) found that during compressive loading, the base of the pedicles underwent the highest amount of strain in the vertebrae. This indicates that the pedicles are an important area of the vertebrae that both undergo, and transmit, a high degree of compression during spinal loading. In our current study, we have identified that vertebrae with Schmorl's nodes tend to have shorter pedicles compared to their healthy counterparts. We hypothesise that the shorter pedicles may not provide adequate buttressing support for the larger, rounder vertebral bodies and that this lack of support may influence vertical herniation of the intervertebral disc (Plomp et al. 2012). This hypothesis requires clinical experimentation to verify the relationship between vertebral shape and vertical intervertebral disc herniation. However, the current results, along with our previous study (Plomp et al., 2012), indicate that vertebral morphology may be an important factor in the aetiology and pathogenesis of Schmorl's nodes.

Dar et al. (2010) have suggested that the amount of torsional movement and the resulting stress on the different spinal segments (thoracic and lumbar) may influence vertical disc herniation and subsequent formation of the Schmorl's node. The strong association found between morphology and pathology in T12 and L1 may indicate the biomechanical importance of vertebral shape at this transition between the thoracic to the lumbar spine (Masharawi et al.,

2004, 2005, 2008; Qui et al., 2006). This suggestion requires further research; however, the results do suggest vertebral morphology as an important area for investigations into back problems in humans.

The present study supports our previous findings (Plomp et al., 2012) looking at the shape of T10-T12 vertebrae, in that particular shape characteristics of the superior vertebral margins are associated with the presence of Schmorl's nodes. It also provides an expansion of the previous findings by indicating that the shape of vertebrae with Schmorl's nodes identified in T10-T12 is similar to that found in L1-L3. The vertebral shape identified in the current study may be the result of a developmental factor, which may eventually predispose vertebrae to vertical disc herniation and Schmorl's nodes due to the influence of vertebral morphology on the overall stability and function of the spine.

The hypothesis that vertebral morphology may play an important role in spinal health is supported by Abbas et al.'s (2010) study on CT scans of 67 clinical patients, who found that in the lower lumbar vertebrae, individuals with degenerative spinal stenosis also had larger anterior-posterior vertebral body diameters. The relationship between vertebral morphology and spinal pathologies, such as disc herniation, disc degeneration, and degenerative spinal stenosis is an avenue of inquiry that may significantly benefit both the clinical and archaeological interpretation and understanding of common back problems.

Conclusion

The results support and extend the findings of our previous study and indicate that the relationship between vertebral morphology and Schmorl's nodes is an area of research which would benefit from further work. A particular morphology seen in T12 and the lumbar spine (L1-

L3) is strongly associated with the presence or absence of Schmorl's nodes. The reason for this relationship remains unclear; however, considering the importance of the role that the pedicles and vertebral body play in spinal stability, it is hypothesized that the shape of these features influences their ability to withstand physical stress. The relatively shorter pedicles identified in this analysis may provide inadequate buttressing for the larger, rounder vertebral bodies. This, in turn, may result in a decrease of the disc's ability to withstand stress during loaded flexion-extension and torsional movements, and lead to the intervertebral disc herniating into the vertebral endplate. Such a hypothesis requires further research, such as 3D analysis of a substantially larger sample size, and clinical experiments on spines with and without Schmorl's nodes, in order to investigate the exact influence vertebral morphology has on spine stability.

Future research will analyze 3D morphology of the entire spine to identify shape variation not seen in 2D analysis. Investigations will also include analysis of 3D images of the spines of patients in order to include information on disc herniations into the spinal canal and the shape of the disc itself. A larger number of skeletal samples, as well as clinical images, will provide further insight into the relationship between vertebral morphology and health in human populations.

Acknowledgments

The authors would like to thank Malin Holst, York Osteoarchaeology, Mike Griffiths Associates, and Field Archaeology Specialists, York for the excavation and initial analysis of the Fishergate House skeletons. We would also like to thank Pre-Construct Archaeology, Jenny Proctor, and James Langthorne, for the excavation, initial skeletal analysis, and access to the Coach Lane skeletons. We also thank Tina Jakob of the Department of Archaeology, Durham University, for the calculation of stature of the Coach Lane individuals. Special thanks go to Durham University for access to the skeletons curated in the Fenwick Human Osteology Laboratory, Department of Archaeology from both these sites, and funding for KAP. The Canadian Centennial Scholarship Fund also provided financial aid during this research, and Helgi Pétur Gunnarsson helped with the analyses. Special thanks to Professor Mark Collard and the Human Evolutionary Studies Program of the Department of Archaeology at Simon Fraser University for support during the

preparation of this manuscript, which was funded by the Social Sciences and Humanities Research Council, Canada Research Chairs Program, Canada Foundation for Innovation, British Columbia Knowledge Development Fund, MITACS, and Simon Fraser University. And finally, we would also like to thank the editor, associate editor, and the two anonymous reviewers for their insightful and helpful comments on early drafts of this paper.

References

Abbas J, Hamoud K, May H, Hay O, Medlej B, Masharawi Y, Peled N, Hershkovitz I. 2010. Degenerative lumbar spine stenosis and lumbar spine configuration. *Eur Spine J* 19: 1865-1873.

Ascádi G, Nemeskéri J. 1970. *History of human life span and mortality*. Akadémiai Kiadó, Budapest.

Adams MA, Dolan P. 2012. Intervertebral disc degeneration: evidence for two distinct phenotypes. *J Anat* 221: 497-506.

Bass WM. 1987. *Human osteology: a laboratory and field manual*. Columbia: Missouri Archaeological Society Special Paper 2

Baylac M, Frieβ M. 2005. Fourier descriptors, Procrustes superimposition, and datadimensionality: An example of cranial shape analysis in modern human populations. In: Slice D, ed. *Modern Morphometrics in Physical Anthropology*. New York: Springer 145-62.

Bienvenu T, Guy F, Coudyze, W, Gilissen E, Roualdes G, Vignaud P, Brunet M. 2011. Assessing endocranial variations in great apes and humans using 3D data from virtual endocasts. *Am J Phys Anthropol* 145: 231-46.

Bookstein F. 1997. Landmark methods for forms without landmarks: Morphometrics of group differences in outline shape. *Med Image Anal* 1(3): 225-43.

Brooks ST, Suchey JM. 1999. Skeletal age determination based on the os pubis: Comparison of the Acsádi-Nemeskéri and Suchey-Brooks methods. *J Hum Evol* 5: 227-38.

Brothwell DR. 1981. *Digging up bones: the excavation, treatment and study of human skeletal remains.* Ithaca, NY: Cornell University Press.

Burke KL. 2012. Schmorl's nodes in an American military population: Frequency, Formation, and Etiology. *J Forensic Sci* 57(3): 571-7.

Cardini A, Nagorsen D, O'Higgins P, Polly PD, Thorington RW, Tongiorgi P. 2009. Detecting biological distinctiveness using geometric morphometrics: An example case from the Vancouver Island Marmot. *Ethol Ecol Evol* 21: 209-23.

Dar G, Peleg S, Masharawi Y, Steinberg N, May H, Hershkovitz I. 2009. Demographic aspects of Schmorl's nodes. *Spine* 34(9): E312-15.

Dar G, Masharawi Y, Peleg S, Steinberg N, May H, Medlej B, Peled N, Gersokovitz I. 2010. Schmorl's nodes distribution in the human spine and its possible etiology. *Eur Spine J* 19: 670-5.

El-Khoury GY, Whitten CG. 1993. Trauma to the upper thoracic spine: Anatomy, biomechanics, and unique imaging features. *Am J Roentgenol* 160(1): 95-102.

Goodall C. 1991. Procrustes methods in the statistical analysis of shape. *J Roy Stat Soc*. Series B 53(2): 285-339.

Harrington JF, Sungarian A, Rogg J, Makker VJ, Epstein MH. 2001. The relation between vertebral endplates shape and lumbar disc herniations. *Spine* 26: 2133-8.

Holst M. 2005. *Fishergate House artefacts and environmental evidence: The human bone*. Arch Planning Consultancy, UK; Accessed online, July 3, 2010.

Hongo M, Abe E, Shimada Y, Murai H, Ishikawa N, Sato K. 1999. Surface strain distribution on thoracic and lumbar vertebrae under axial compression: the role in burst fractures. *Spine* 24: 1197-1202.

Işcan MY, Loth SR, Wright RK. 1984. Age estimation from the rib by phase analysis: White males. *J Forensic Sci* 29: 1094–104.

Işcan MY, Loth SR, Wright RK. 1985. Age estimation from the rib by phase analysis: White females. *J Forensic Sci* 30: 853–63.

Kimmerle EH, Ross A, Slice D. 2008. Sexual dimorphism in America: Geometric morphometric analysis of the craniofacial region. *J Forensic Sci* 53(1): 54-7.

Klingenberg CP. 2011. MorphoJ: an integrated software package for geometric morphometrics. *Mol Ecol Res* 11: 353–357.

Knūsel, C.J., S. Göggel, & D. Lucy. 1997. Comparative Degenerative Joint Disease of the Vertebral Column in the Medieval Monastic Cemetery of the Gilbertine Priory of St. Andrew, Fishergate, York, England. *American Journal of Physical Anthropology* 103: 481-495.

Kovarovic K, Aiello LC, Cardini A, Lockwood CA. 2011. Discriminant function analyses in archaeology: are classification rates too good to be true? *J Arch Sci* 38: 3006-18.

Langthorne JY. 2012. *Human Skeletal Remains in Goode A, Taylor-Wilson R. Archaeological exhumation of the former Quaker burial ground on Coach Lane, North Shields, North Tynside, Tyne and Wear: Assessment Report*: pp 44-65.

Letić M. 2012. Feeling wall tension in an interactive demonstration of Laplace's law. Advances in Physiology Education 36(2): 176.

Lieberman DE, Carlo J, Ponce de León M, Zollikofer CP. 2007. A geometric morphometrics analysis of heterochrony in the cranium of chimpanzees and bonobos. *J Hum Evol* 52: 647-62.

Lovejoy CO, Meindl RS, Pryzbeck TR, Mensforth RP. 1985. Chronological metamorphosis of the auricular surface of the ilium: A new method for the determination of age at death. *Am J Phys Anthropol* 68: 15–28.

Masharawi Y, Rothschild B, Dar G, Peleg S, Robinson D, Been E, Hershkovitz I. 2004. Facet orientation in the thoracolumbar spine. *Spine* 29(16): 1755-63.

Masharawi Y, Rothschild B, Salame K, Dar G, Peleg S, Hershkovitz I. 2005. Facet tropism and interfacet shape in the thoracolumbar vertebrae: Characterizations and biomechanical interpretation. *Spine* 30(11): E281-92.

Masharawi Y, Salame K, Mirovsky Y, Peleg S, Dar G, Steinberg N, Hershkovitz I. 2008. Vertebral body shape variation in the thoracic and lumbar spine: Characterization of its asymmetry and wedging. *Clin Anat* 21: 46-54.

Mok F, Samartzis D, Karppinen J, Luk KD, Fong DY, Cheung KM. 2010. Prevalence, determinants, and association of Schmorl's nodes of the lumbar spine with disc degeneration: A population-based study of 2449 Individuals. *Spine* 35(21): 1944-52.

Neubauer S, Gunz, P, Hublin JJ. 2009. The patterns of endocranial ontogenetic shape changes in humans. *J Anat* 215: 240-55.

Neubauer S, Gunz P, Hublin JJ. 2010. Endocranial shape changes during growth in chimpanzees and humans: A morphometric analysis of unique and shared aspects. *J Hum Evol* 59:555-66.

Novak M, Šlaus M. 2011. Vertebral pathologies in two early modern period (16^{th}-19^{th} Century) populations from Croatia. *Am J Phys Anthropol* 145: 270-81.

O'Higgins P, Jones N. 1998. Facial growth in Cerocebus torquatus: An application of three-dimensional geometric morphometric techniques to the study of morphological variation. *J Anat* 193: 251-272.

O'Higgins P, Jones N. 2006. Morphologika: Tools for statistical shape analysis. Hull York Medical School.

Peloquin JM, Yoder JH, Jacobs NT, Moon SM, Wright AC, Elliot DM. 2014. Human L3L4 intervertebral disc mean 3D shape, modes of variation, and their relationship to degeneration. *J Biomech* 47(10): 2452-2459.

Pfirrmann C, Resnick D. 2001. Schmorl's nodes of the thoracic and lumbar spine: Radiographic-pathologic study of prevalence, characterization, and correlation with degenerative changes of 1,650 spinal levels in 100 cadavers. *Radiology* 219: 368-74.

Phenice TW. 1969. A newly developed visual method of sexing the os pubis. *Am J Phys Anthropol* 30: 297–302

Plomp, K.A., Roberts, C.A., Strand Viðarsdóttir, U., 2012. Vertebral morphology influences the development of Schmorl's nodes in the lower thoracic vertebrae. *Am J Phys Anthropol* 149(4): 572-582.

Qui TX, Teo EC, Zhang QH. 2006. Comparisons of kinematics between thoracolumbar T11-T12 and T12-L1 functional spinal units. *J Eng Med* 220: 493-504.

R Development Core Team. R: A language and environment for statistical computing. R Foundation for Statistical Computing Vienna, Austria. ISBN 3-900051-07-0, URL http://www.R-project.org; 2012

Robb J, Bigazzi R, Lazzarini L, Scarsini C, Sonego F. 2001. Social "status" and biological "status": A comparison of grave goods and skeletal indicators from Pontecagnano. *Am J Phys Anthropol* 115: 213-22.

Rohlf FJ. 2004. Version 1.40. Ecology and Evolution, SUNY at Stony Brook.

Rohlf FJ. 2003. Bias and error in estimates of mean shape in geometric morphometrics. *J Hum Evol* 44: 665-83.

Rohlf FJ, Slice D. 1990. Extensions of the Procrustes method for the optimal superimposition of landmarks. *Syst Zool* 39(1): 40-59.

Schmorl G, Junghans H. 1971. *The human spine in health and disease*. New York: Grune & Stratton.

Shapiro L. 1993a. Evaluation of the "unique" aspects of human vertebral bodies and pedicles with consideration of *Australopithecus africanus*. *J Hum Evol* 25: 433-470.

Shapiro L. 1993b. Functional morphology of the vertebral column in primates. In: Gebo DL: *Postcranial adaptation in non-human primates.* Dekalb, Illinois: Nothern Illinois University Press.

Slice DE. 2007. Geometric morphometrics. *Annu Rev Anthropol* 36: 261-81.

SPSS Inc. 2007. SPSS Base 8.0 for Windows User's Guide. Chicago: SPSS Inc.

Trotter M, Gleser GC. 1958. A re-evaluation of estimation of stature based on measurements of stature taken during life and of long bones after death. *Am J Phys Anthropol* 16(1): 79-123.

Üstündağ H. 2009. Schmorl's nodes in a Post-Medieval skeletal sample from Klostermarienberg, Austria. *Int J Osteoarchaeol* 19: 695-710.

Von Forell GA, Nelson TG, Samartzis D, Bowden AE. 2014. Changes in vertebral strain energy correlate with increased presence of Schmorl's nodes in multi-level lumbar disk degeneration. *J Biomech Engin* 136: 061002-1-6.

White JW, Ruttenberg BI. 2007. Discriminant function analysis in marine ecology: Some oversights and their solutions. *Mar Ecol Prog* 329: 301-5.

Whyne CM, Hu SS, Klisch S, Lotz J. 1998. Effect of the pedicle and posterior arch on vertebral body strength predictions in finite element modeling. *Spine* 23(8): 899-907.

Williams FMK, Manek NJ, Sambrook PN, Spector TD, Macgregor AJ. 2007. Schmorl's nodes: Common, highly a, and related to lumbar disc disease. *Arthritis Rheum* 57(5): 855-60.

Zelditch ML, Swiderski DL, Sheets HD. 2004. *Geometric morphometrics for biologists: A primer*. San Diego, CA: Elsevier Academic Press.

Figure 1) Map of England illustrating location of skeletal collections used in this analysis from Fishergate House, York, and Coach Lane, North Shields, Tyne and Wear.
217x248mm (300 x 300 DPI)

Figure 2) Vertebrae displaying Schmorl's nodes.
116x47mm (300 x 300 DPI)

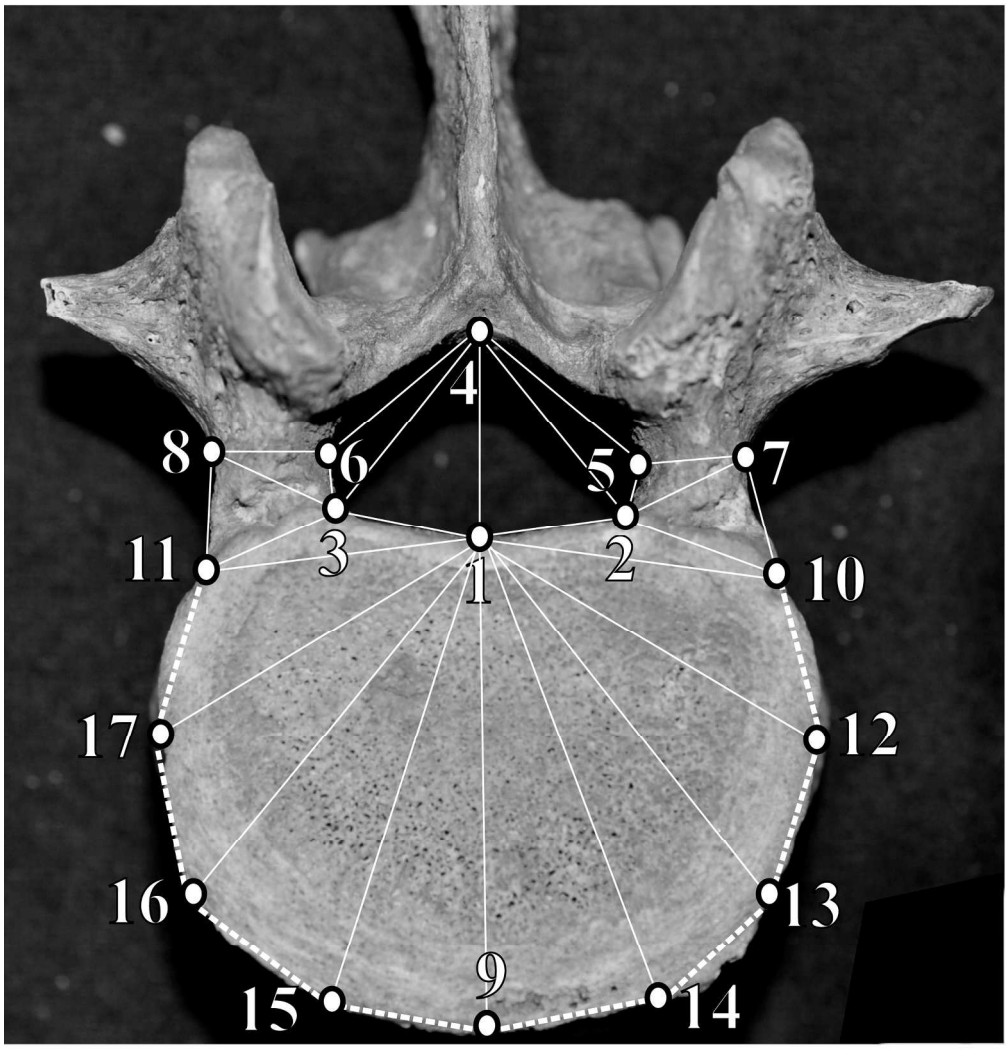

Figure 3) Location of landmarks used for shape analysis. Landmarks 1 through 17 are analyzed in the first dataset, and landmarks 1 through 8, which focus on the neural canal and pedicles, are included in the second dataset.
202x211mm (300 x 300 DPI)

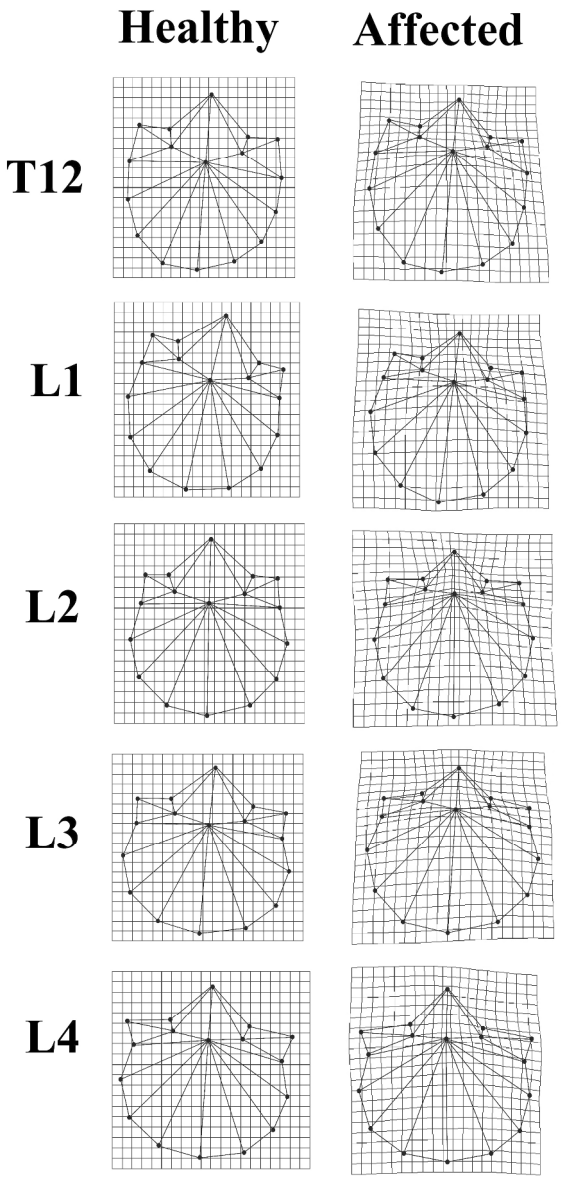

Figure 4) Wireframe images representing the mean morphology of healthy and affected vertebrae. Thin-plate splines illustrate the area of deformation in morphology from the healthy to the affected vertebrae; the deformation of the grids has been multiplied by 2 for ease of interpretation.
185x355mm (300 x 300 DPI)

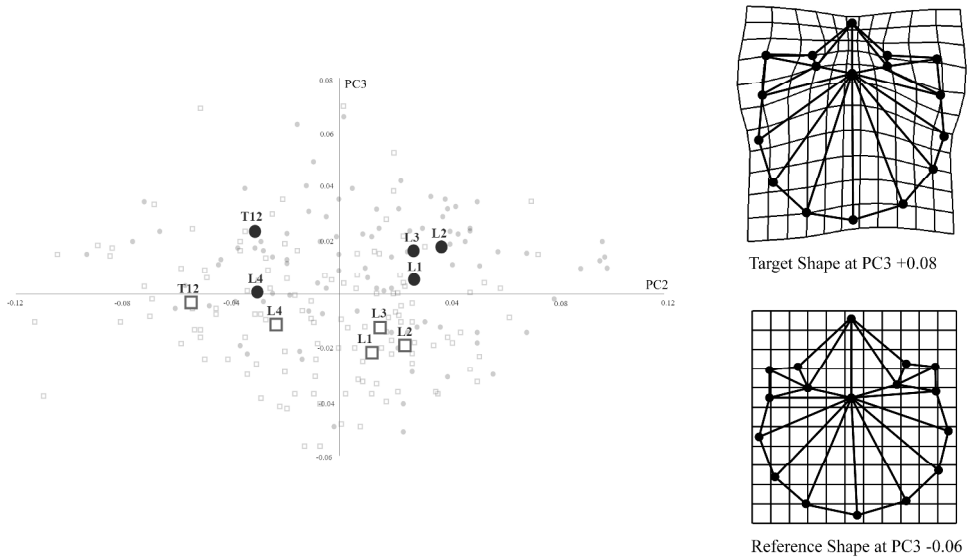

Figure 5) PCA chart illustrating shape variability of vertebrae on PC2 and PC3, representing 36.8% of the total variance (open squares – healthy, filled circles – affected). The larger symbols represent the means of each group of vertebrae. Affected and healthy vertebrae separate on a combination of PC2 and PC3. Wireframes illustrate shape differences occurring along PC3, with the reference shape (bottom) set at PC3 -0.06 and the target shape (top) at PC3 +0.08.
482x274mm (300 x 300 DPI)

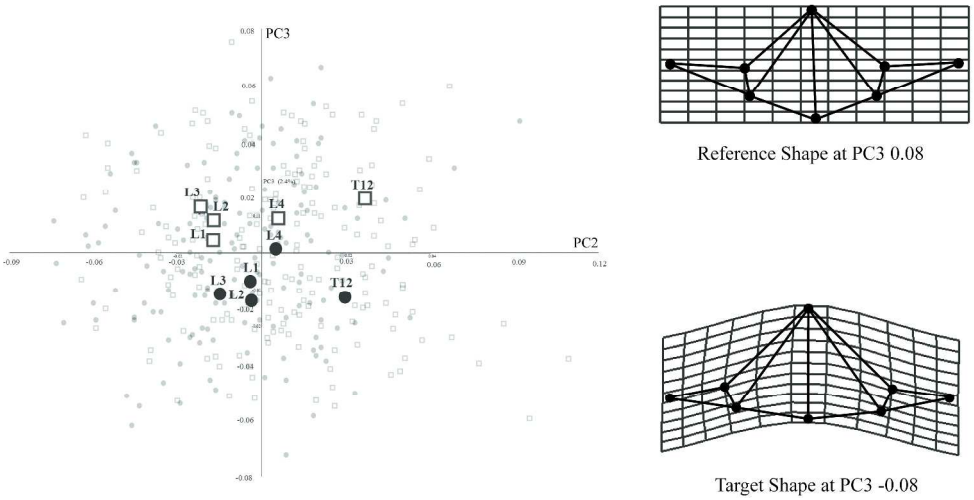

Figure 6) PCA chart illustrating shape variability of vertebrae on PC2 and PC3, representing 6.1% of the total variance (open squares – healthy, filled circles – affected). The larger symbols represent the means of each group of vertebrae. Wireframes illustrate shape differences occurring along PC3, with the reference shape (top) set at PC3 +0.08 and the target shape (bottom) at PC3 -0.08. The wireframes represent the variation within the 8 landmark dataset, and although the difference in landmark count results in a different shape of deformation grid, the morphological differences occurring are consistent with those identified in the full landmark set.
437x224mm (300 x 300 DPI)

Table 1) Number of individuals studied, with sex [male, female, undetermined (U)] and age indicated [YA = young adult (18-25 years), MA = middle adult (26-45years), OA = old adult (46+ years), U = unknown age], included in the analysis. Age categories based on Buikstra and Ubelaker (1994).

Site	**Period**	**Reference**	♀	♂	**U**	**YA**	**MA**	**OA**	**U**	**Inds**
Fishergate House, York, Yorkshire	Medieval (12^{th}-16^{th} C AD)	Holst 2005	23	33	3	13	25	19	2	59
Coach Lane, North Shields Tyne and Wear	Post-Medieval (1711-1857 AD)	Langthorne 2012	12	16	3	11	13	5	2	31
Total			**35**	**49**	**6**	**24**	**38**	**24**	**4**	**90**

Table 2) Summary of study 'materials' by vertebral segment, sex, and vertebral status. Due to differential preservation of landmarks on the vertebrae, two datasets were analyzed: one with 17 landmarks, the other limited to eight landmarks.

			17 Landmarks			8 Landmarks	
Fishergate House							
		Healthy	**Affected**	**Total**	**Healthy**	**Affected**	**Total**
T12	Males	5	4	**9**	10	13	**23**
	Females	3	5	**8**	8	12	**20**
	Unknown	0	1	**1**	0	1	**1**
L1	Males	9	4	**13**	12	8	**20**
	Females	7	6	**13**	11	12	**23**
	Unknown	0	2	**2**	0	2	**2**
L2	Males	3	7	**10**	7	12	**19**
	Females	3	4	**7**	11	11	**22**
	Unknown	0	2	**2**	0	2	**2**
L3	Males	5	7	**12**	9	15	**24**
	Females	6	5	**11**	8	9	**17**
	Unknown	0	1	**1**	0	2	**2**
L4	Males	9	3	**12**	17	8	**25**
	Females	6	2	**8**	14	9	**23**
	Unknown	1	1	**2**	3	0	**3**
Coach Lane							
T12	Males	6	9	**15**	5	11	**16**

	Females	6	3	**9**	7	2	**9**
	Unknown	1	0	**1**	1	0	**1**
L1	Males	6	9	**15**	6	9	**15**
	Females	10	0	**10**	11	0	**11**
	Unknown	2	0	**2**	2	0	**2**
L2	Males	4	7	**11**	8	8	**16**
	Females	8	1	**9**	10	1	**11**
	Unknown	2	0	**2**	2	0	**2**
L3	Males	4	7	**11**	6	10	**16**
	Females	9	2	**11**	9	3	**12**
	Unknown	0	0	**0**	1	2	**3**
L4	Males	2	7	**9**	6	9	**15**
	Females	8	1	**9**	10	2	**12**
	Unknown	2	0	**2**	2	0	**2**

Table 3) Summary of vertebrae correctly identified as 'healthy' or 'affected' from the DFA with cross-validation, based on 17 landmarks for each vertebra, with the number of PCs and total variance for each.

	DFA Scores			PCs
	Affected	**Healthy**	**Total**	**Total Variance**
T12	76.2 %	85.7 %	81.0 %	11 PCs = 95.38 %
L1	71.4 %	82.4 %	78.2 %	25 PCs = 99.98 %
L2	71.4 %	75.0 %	73.2 %	3 PCs = 74.74 %
L3	69.6 %	73.9 %	71.7 %	4 PCs = 80.82 %
L4	78.6 %	64.3 %	69.0 %	17 PCs = 99.12%

Table 4) Summary of MANOVA scores (Wilks lambda λ, F-ratio, p-value) of PC values for all vertebrae in both sets of landmarks.

	17 landmarks	8 landmarks
T12	λ 0.436 F= 3.523 p = 0.003*	λ 0.644 F= 11.983 p = 0.000*
L1	λ 0.271 F= 3.114 p = 0.002*	λ 0.588 F= 2.700 p = 0.000*
L2	λ 0.660 F= 6.365 p = 0.001*	λ 0.650 F= 5824 p = 0.000*
L3	λ 0.786 F= 2.794 p = 0.038*	λ 0.837 F= 4.559 p = 0.006*
L4	λ 0.431 F= 1.862 p = 0.080	λ 0.630 F= 4.129 p = 0.005*

* indicates significant value

Table 5) Summary of "correctly identified" affected and healthy vertebrae from the DFA with cross-validation based on eight landmarks of the neural canal and pedicles for each vertebra with the number of PCs included and total variance for each.

	DFA Scores			PCs
	Affected	Healthy	Total	% Total Variance
T12	76.3 %	74.2 %	75.4 %	3 PCs = 78.5%
L1	70.9 %	76.2 %	73.9 %	9 PCs = 97.9 %
L2	76.5 %	75.0 %	72.2 %	1 PC = 59.9%
L3	75.6 %	69.7 %	73.0%	14 PCs = 100.0%
L4	63.0%	60.4 %	60.0 %	5 PCs = 90.0 %